




# Evaluation of pounding effects between reinforced concrete frames subjected to far-field earthquakes in terms of damage index

S. H. Hosseini<sup>1</sup> · H. Naderpour<sup>1</sup> · R. Vahdani<sup>1</sup> · R. Jankowski<sup>2</sup> 

Received: 28 April 2021 / Accepted: 13 October 2021  
© The Author(s) 2021

## Abstract

In this paper, three different damage indexes were used to detect nonlinear damages in two adjacent Reinforced Concrete (RC) structures considering pounding effects. 2-, 4- and 8-story benchmark RC Moment Resisting Frames (MRFs) were selected for this purpose with 60%, 75%, and 100% of minimum separation distance and also without any in-between separation gap. These structures were analyzed using the incremental dynamic analysis method under 44 far-field ground motion records. Comparison of the results between the MRFs with and without considering pounding effects show that collisions lead to a decrease in the values of coefficient of determination and the nonlinear damage occurs in lower seismic intensity. As a result, using the damage indexes, nonlinear damages can be detected during a specific seismic intensity. Moreover, considering a minimum separation distance leads to an increase in the coefficient of determination between the damage index and the maximum story drift ratio. Furthermore, due to pounding, shorter MRFs are damaged more significantly than the taller structures.

**Keywords** Reinforced concrete moment resisting frames · Structural pounding · Far-field earthquakes · Incremental dynamic analysis · Maximum story drift ratio · Damage index

## 1 Introduction

Structural pounding due to insufficient gaps may cause collisions between adjacent structures during earthquakes. If adjacent buildings, or bridge segments, are not separated suitably from each other, impact forces may cause serious damages even if structures are well designed (Miari et al. 2019, 2021; Rezaei et al. 2020). The first research work that explains possible dangers due to building pounding was performed by Anagnostopoulos (1988). Several reports showed that at least 15% of buildings were damaged due to the impact of

---

✉ R. Jankowski  
jankowr@pg.edu.pl

<sup>1</sup> Faculty of Civil Engineering, Semnan University, Semnan, Iran

<sup>2</sup> Faculty of Civil and Environmental Engineering, Gdansk University of Technology, ul. Narutowicza 11/12, 80-233 Gdansk, Poland

adjacent buildings during the 1985 Mexico City earthquake (Rosenblueth and Meli 1986). Researchers used different numerical and experimental methods to simulate the problem of earthquake-induced pounding between adjacent buildings (Leibovich et al. 1996; Ruangrassamee and Kawashima 2001; DesRoches and Muthukumar 2002; Mahmoud and Jankowski 2009; Jankowski 2010; Yaghmaei-Sabegh and Jalali-Milani 2012; Barros et al. 2013; Softysik and Jankowski 2013; Naderpour et al. 2015; 2016; 2017; Kazemi et al. 2021a). A number of investigations were focused on comparison between different numerical models of pounding force during impact (see Mahmoud, et al. 2008; Muthukumar and DesRoches 2006, for example). Other studies concerned the experimental verification of the effectiveness of pounding force models in simulation of earthquake-induced structural interactions (Barros and Khatami 2013; Khatiwada et al. 2013). Some recent analyses were also focused on different pounding mitigation methods so as to reduce the negative effects of collisions during seismic excitations (see Kandemir-Mazanoglu and Mazanoglu 2017; Elwardany et al. 2021, for example).

A new equation to calculate the effective periods of inelastic buildings, based on ductility demand, which can be successfully applied for the determination of a minimum separation gap was proposed by Khatami et al. (2019). The results showed that using the proposed methods, the impacts between two adjacent buildings due to earthquake-induced structural pounding can be prevented by ensuring sufficient minimum separation gap. A new model for calculating impact force and energy dissipation, based on the coefficient of restitution and impact velocity, was proposed by Naderpour and Khatami (2015). To evaluate the accuracy of the suggested formula, the relationship between the selected coefficient of restitution and the calculated coefficient of restitution was compared. The results showed good accuracy in comparison with other formulas. A review of earthquake-induced pounding between adjacent buildings considering identification of parameters and soil-structure interaction issues was performed by Miari et al. (2019). The effects of pounding on fixed-base and base-isolated buildings were also examined. Based on the obtained results, directions of future research studies on structural pounding were recommended. The effect of the infill panels on the seismic pounding response of adjacent structures in series was studied by Elwardany et al. (2017, 2019). The results of the analysis showed that the existence of infill panels changes the seismic behavior of the structures during pounding under seismic excitation. The effect of using linear and nonlinear fluid viscous dampers on the seismic collapse capacities of adjacent structures prone to pounding was investigated by Kazemi et al. (2021b). The results demonstrated that the existence of dampers can substantially improve the seismic behavior of structures having a significant influence on their collapse capacities. The effects of pounding between two L-shaped asymmetric steel buildings under earthquake excitation were evaluated by Softysik and Jankowski (2016). The results indicated that these effects lead to both an increase and/or a decrease in the structural response. Moreover, torsional vibrations (due to eccentric pounding) were found to play an important role in the overall pounding-involved response of asymmetric steel buildings under earthquake excitations. Building damage due to structural pounding during earthquakes was studied by Softysik and Jankowski (2015). Steel asymmetric structures with a different number of stories were utilized for numerical analysis. Three-dimensional gap-friction elements were used for controlling pounding between buildings. The acceleration time histories of the El Centro earthquake were used in the numerical analysis. The results of the study clearly showed that pounding may substantially influence the response of steel buildings intensifying their damage during earthquakes. The influence of non-uniform earthquake excitation on the pounding-involved response of two buildings using non-linear FEM analysis was investigated by Jankowski (2012). The obtained results showed



that the non-uniform ground motion excitation may considerably influence the pounding-involved behavior of buildings. The effect of different structural configurations on pounding-involved response of adjacent planar Reinforced Concrete (RC) building frames subjected to strong ground motions was examined by Efraimiadou et al. (2013a). The results showed that the effect of collisions of adjacent frames is unfavorable for most of the cases and, as a result, the structural pounding phenomenon is rather detrimental than beneficial. The effect of collisions between adjacent RC building frames under multiple earthquakes was investigated by Efraimiadou et al. (2013b). The effects of various parameters, such as maximum horizontal displacement of the top floor, ductility of columns, permanent displacements, and four different separation gaps, were considered. Based on the results, the behavior of adjacent structures was found to be strongly affected by multiple earthquakes and, for most of the cases, the seismic sequences appeared to be detrimental in comparison with the single seismic events. A new damage index for plane steel frames considering the strength and stiffness degradation under ground motion was proposed by Kamaris et al. (2013). Various parameters, including interaction between the axial force and the bending moment with low-cycle fatigue, were examined. The correlation of the proposed damage index showed good match with five well known indexes described in the literature. The accuracy of four different criteria to calculate the separation necessary to prevent seismic pounding between nonlinear hysteretic structural systems was evaluated by Lopez-Garcia and Soong (2009b). The results showed that the Double Difference Combination (DDC) rule is always more accurate than the Square Root of the Sum of the Squares (SRSS) rule in the case of linear systems. However, in the case of nonlinear hysteretic systems, none of the four implementations of the DDC rule was consistently more accurate than the SRSS rule. The accuracy of the DDC rule to predict the separation gap necessary to prevent seismic pounding between linear structural systems was examined by Lopez-Garcia and Soong (2009a). Damage assessment of adjacent buildings under earthquake loads, using input energy, dissipated energy, and damage indexes, was studied by Moustafa and Mahmoud (2014). Numerical examples of damage of fixed-base and base-isolated adjacent buildings with elastic–plastic force–deformation relation were considered. A probabilistic risk assessment for seismic pounding with efficient application to linear systems was performed by Tubaldi et al. (2012). To reduce the pounding probability of adjacent buildings, the proposed method was analyzed using viscous dampers and their capability was evaluated. The results obtained were validated against purely numerical simulation results.

The current research is focused on damage assessment in adjacent RC Moment Resisting Frames (MRFs) considering pounding effects under ground motion records. For this purpose, some illustrative benchmark structures, including 2- and 4-story as well as 4- and 8-story RC MRFs, were examined based on three damage indexes, i.e. Park and Ang index (Park and Ang 1985), modified Park and Ang damage index proposed by Kunnath et al. (1992) and Consenza et al. index (Cosenza et al. 1993).

## 2 Nonlinear modeling of structures

In this research, the 2-, 4- and 8-story RC MRFs, designed by Haselton and Deierlein (2005), were used. Each of the buildings was designed according to the IBC (2003), ASCE7-02 (2002), and ACI 318-02 (2002) (see Haselton and Deierlein 2005). In these models, three-dimensional effects and uncertainty in modeling were used (Deierlein and Haselton 2005). Also, deterioration modes that participated in the sideways



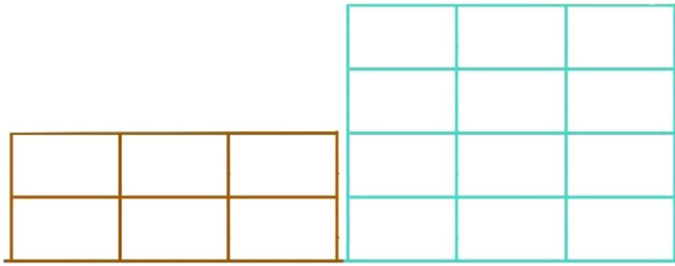


**Fig. 1** Elevation views of the 2- and 4-story RC MRFs under consideration

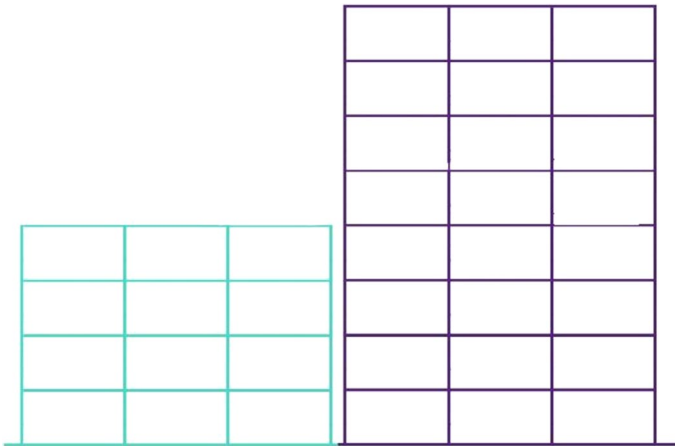


**Fig. 2** Elevation views of the 4- and 8-story RC MRFs under consideration

collapse were considered using the element model developed by Ibarra and Krawinkler (2005) and Ibarra et al. (2005). In this regard, OpenSees software (McKenna et al. 2010) was used (Altoontash 2004). The elevation views of the 2-, 4- and 8-story RC MRFs, including geometry and dimensions, are presented in Fig. 1 and Fig. 2, respectively. The *P*-Delta effect was modeled using the concept of leaning column. The modified Ibarra-Krawinkler bilinear-hysteretic model, as a nonlinear rotational spring, was considered for deteriorating moment-rotation hysteresis (Lignos and Krawinkler 2010). Moreover, an elastic beam-column element in the middle and two zero-length elements located at both ends were also used in the model. In other words, in order to compute the damage indexes, the modified Ibarra-Medina-Krawinkler bilinear hysteretic model (IMK model) was implemented (see Ibarra et al. 2005) by applying a nonlinear rotational spring at both ends of each beam element and at both ends of each column element. Therefore, the relation between the moment and rotation  $M$ - $\theta$  for each hinge could be obtained, and finally, having the  $M$ - $\theta$  relation for each story, the damage indexes could be computed (Mohebi et al. 2019).



### 3 Modeling of pounding

In this study, to model the pounding phenomenon, the linear viscoelastic contact model (Kelvin-Voigt model) was employed using OpenSees software (McKenna et al. 2010). Pounding force in each story was obtained based on the following equation (Anagnostopoulos 1988):

$$F(t) = K_{imp}\delta(t) + C_{imp}\dot{\delta}(t) \tag{1}$$

where  $K_{imp}$  is the impact spring's stiffness coefficient,  $\delta(t)$  is the interpenetration depth,  $C_{imp}$  is the impact damping coefficient, and  $\dot{\delta}(t)$  is the relative velocity of pounding floors, respectively. The value of damping coefficient can be obtained as follows (Anagnostopoulos 1988):

$$C_{imp} = 2\xi\sqrt{K_{imp}\frac{m_i m_j}{m_i + m_j}} \tag{2}$$

$$\xi = \frac{-\ln(e)}{\sqrt{\pi^2 + (\ln(e))^2}} \tag{3}$$

where  $\xi$  is the impact damping ratio,  $e$  is the coefficient of restitution, and  $m_i$  and  $m_j$  are masses of two colliding structures. It was considered in the analysis that impact occurs at the story levels (slab-to-slab pounding). The coefficient of restitution accounts for the energy dissipation during impact due to such effects as plastic deformations, local cracking and friction, etc. (Goldsmith 1960). This parameter for concrete-to-concrete impact was assumed to be 0.65 (Mahmoud and Jankowski 2011; Anagnostopoulos and Karamaneas 2008). The impact stiffness coefficient depends mainly on the material characteristics of the colliding structures and the geometry at the vicinity of impact. Assuming that the contact geometry is taken into account with the use of the area of the overlapping region instead of the indentation depth, the impact stiffness coefficient should be directly related to the modulus of elasticity of the colliding structures. The equations proposed by Polycarpou et al. (2014) were used to determine the impact stiffness coefficient:

$$K_{imp} = \left[ \frac{1 - \nu_1^2}{E_{Dynamic,1}} + \frac{1 - \nu_2^2}{E_{Dynamic,2}} \right]^{-1} \tag{4}$$

$$E_{Dynamic,i} = 5.82(E_{Static,i})^{0.63}, \text{ in GPa} \tag{5}$$

where  $\nu_i$  is the Poisson's ratio,  $E_{Dynamic,i}$  is the dynamic elastic modulus of normal strength concrete,  $E_{Static,i}$  is the static elastic modulus for structure  $i$  that is calculated from the stress-strain diagram. The dynamic elastic modulus is used primarily to evaluate the soundness of concrete in durability tests; it is a more appropriate value when concrete is to be used in structures subjected to dynamic loading, i.e. impact or earthquake (Al-Amawee and Salman 2006). In this study, the static elastic modulus and the Poisson's ratio were assumed to be equal to 21 GPa and 0.2, respectively. In order to investigate the effect of separation distance on the seismic pounding of adjacent structures, separation distance equal to zero as well as equal to a minimum separation distance,  $\delta_{MT}$ , as calculated



according to the ASCE seismic provision, was considered. Each pounding model was analyzed for two aforementioned separation distances and compared to the case when structures vibrate independently (without any adjacent structure).

### 4 Incremental dynamic analysis

Incremental Dynamic Analysis (IDA) is a technique to assess the seismic collapse capacities of structures utilizing a series of nonlinear dynamic analyses. Modern design provisions, such as FEMA P695 (2009), propose a set of 44 ground motions to be used in the analysis. This is done to take into account the record to record variability. Also, recent literature (see Baltzopoulos et al. 2019, for example) suggests that the number of records used can be kept in the 40 to 100 range and achieve 10% mean relative error. Therefore, in the current research, a set of 44 far-field ground motion records presented in FEMA P695 (2009) were used to perform IDAs (see Table 1). Figure 3a and b present the IDA curves (color curves) and their corresponding median (black curves) for the 4- and 8-story RC pounding structures, respectively, with the separation distance equal to zero.

### 5 Implementation of damage indexes

In order to present the damage level numerically, it is necessary to select a practical Damage Index (*DI*). Using a proper *DI*, the local status of an element or the overall state of a structure after an earthquake loading can be determined. Application of *DIs* in damage detection of structures was studied by several researchers (Sharifi et al. 2012; Alhaddad et al. 2015; Nie et al. 2017; Pang et al. 2018; Huang et al. 2018). In this research work, three *DIs* proposed by Park and Ang (1985), Cosenza et al. (1993), and Kunnath et al. (1992) were selected to evaluate structural pounding damage in adjacent RC MRFs, which are considered as local *DIs*. As a matter of fact, a *DI* is local when it refers to a single point, section, member, or structural part, whereas it is considered to be global when it defines the state of the entire structure (Hanganu et al. 2002). Then, a global *DI* is obtained through special combinations using weighted factors of local *DIs*. The weighting factor for any story can be related to the magnitude of its corresponding *DI*. On the other hand, a story with severe damage is a candidate for the bigger weight (Ghobarah et al. 1999). Weighted averaging methods were proposed by Park and Ang (1985) and Bracci et al. (1989) to integrate damage of single elements for each individual story. Park and Ang (1985) suggested a damage index which is based on deformation and energy concepts in structural elements, so as to achieve the damage level in each story and the overall structure based on Eq. (6) and Eq. (7), respectively:

$$DI_{\text{story}} = \sum_{i=1}^n (\lambda_{i,\text{component}} \cdot DI_{i,\text{component}}) \tag{6}$$

$$DI_{\text{overall}} = \sum_{i=1}^n \left\{ (\lambda_i)_{\text{story}} (DI_i)_{\text{story}} \right\} \tag{7}$$

where

**Table 1** The forty-four ground motions of the FEMA P695 far-field set (FEMA P695 (2009))

No.	Event	Date	Mw	Station	Closest Fault Dis- tance (km)	Orientation	A <sub>g</sub> (g)	V <sub>g</sub> (cm/s)
1	Manjil, Iran	1990/06/20	7.4	Abbar	12.6	Long	0.515	42.5
2						Trans	0.496	52.1
3	Kocaeli, Turkey	1999/08/17	7.4	Arcelik	17.7	000	0.218	17.7
4						090	0.149	39.5
5	Friuli, Italy	1976/05/06	6.5	Tolmezzo	37.7	000	0.351	22
6						270	0.315	30.8
7	Superstition Hills, CA	1987/11/24	6.7	El Centro Imp.Co. Center	13.9	000	0.358	46.4
8						090	0.258	40.9
9	Duzce, Turkey	1999/11/12	7.1	Bolu	17.6	000	0.728	56.4
10						090	0.822	62.1
11	Superstition Hills, CA	1984/11/24	6.7	Poe Road	12.4	270	0.446	35.7
12						360	0.30	32.8
13	Loma Prieta, CA	1989/10/18	6.9	Capitola	14.5	000	0.529	36.5
14						090	0.443	29.3
15	Chi-Chi, Taiwan	1999/09/20	7.6	CHY101	11.1	W	0.353	70.6
16						N	0.440	115
17	Landers, CA	1992/07/23	7.3	Coolwater	21.2	Long	0.283	25.6
18						Trans	0.417	42.3
19	Kocaeli, Turkey	1999/08/17	7.4	Duzce	12.7	180	0.312	58.8
20						270	0.358	46.4
21	Loma Prieta, CA	1989/10/18	6.9	Gilroy Array #3	14.4	000	0.555	35.7
22						090	0.367	44.7
23	Imperial Valley, CA	1979/10/15	6.5	Delta	43.6	262	0.238	26
24						352	0.351	33

Table 1 (continued)

No.	Event	Date	Mw	Station	Closest Fault Dis- tance (km)	Orientation	$A_g$ (g)	$V_g$ (cm/s)
25	Imperial Valley, CA	1979/10/15	6.5	El Centro Array #11	12.6	140	0.364	34.5
26						230	0.380	42.1
27	Hector Mine, CA	1999/10/16	7.1	Hector	11.7	000	0.266	28.6
28						090	0.337	41.7
29	Northridge, CA	1994/01/17	6.7	Canyon County—W Lost Canyon	13	000	0.410	43
30						270	0.482	45.1
31	Northridge, CA	1994/01/17	6.7	Beverly Hills—14,145 Mulholland	19.6	009	0.416	59
32						279	0.517	62.8
33	Kobe, Japan	1995/01/16	6.9	Nishi—Akashi	11.1	000	0.509	37.3
34						090	0.503	36.6
35	San Fernando, CA	1971/02/09	6.6	LA Hollywood Stor Lot	21.2	090	0.210	18.9
36						180	0.174	14.9
37	Cape Mendocino, CA	1992/04/25	7.1	Rio Dell Overpass	18.5	270	0.385	43.9
38						360	0.549	42.1
39	Kobe, Japan	1995/01/16	6.9	Shin-Osaka	15.5	000	0.243	37.8
40						090	0.212	27.9
41	Chi-Chi, Taiwan	1999/09/20	7.6	TCU045	24.1	W	0.474	36.7
42						N	0.512	39
43	Landers, CA	1992/06/28	7.3	Yermo Fire Station	24.9	270	0.245	51.5
44						360	0.152	29.7



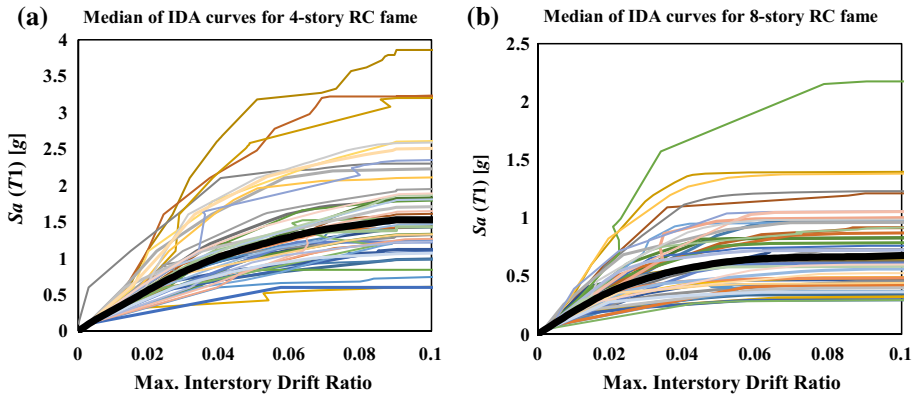


**Fig. 3** IDA curves of the considered benchmark pounding structure with separation distance equal to 0 under 44 far-field ground motion records: **a** 4-story building, **b** 8-story building

$$(\lambda_i)_{\text{component}} = \left[ \frac{E_i}{\sum_{k=1}^n E_i} \right]_{\text{component}} \tag{8}$$

$$(\lambda_i)_{\text{story}} = \left[ \frac{E_i}{\sum_{k=1}^n E_i} \right]_{\text{story}} \tag{9}$$

It should be added that  $E$  in Eq. (8) denotes the total energy dissipated by the element and  $n$  is the number of elements of an individual story, whereas,  $E$  in Eq. (9) represents the total energy absorbed by the story and  $n$  is the number of stories.

The  $DI$  proposed by Cosenza et al. (1993) is presented by Eq. (10) as follows:

$$DI = \frac{\mu - 1}{\mu_{u,mon} - 1} \tag{10}$$

where  $\mu$  is the maximum ductility during the history of loading and  $\mu_{u,mon}$  is the maximum allowable value of ductility, which is equal to  $u_{u,mon}/u_y$ . It should be noted that  $u_{u,mon}$  is the ultimate displacement under monotonic loading and  $u_y$  is the yield displacement. For flexure-resisting components,  $\mu$ ,  $\mu_{u,mon}$ ,  $u_{u,mon}$ , and  $u_y$  are replaced with  $\mu_\theta$ ,  $\mu_{\theta,mon}$ ,  $\theta_{u,mon}$ , and  $\theta_y$ , respectively. Moreover,  $\mu_\theta$  is the rotation ductility during the loading history and  $\mu_{\theta,mon}$  is the maximum allowable value of rotation ductility under monotonic loading, while  $\theta_{u,mon}$  and  $\theta_y$  are the ultimate and the yield rotation, respectively. The damage index proposed by Park and Ang (1985) was extended and modified by Kunnath et al. (1992) using both deformation and hysteretic energy as follows:

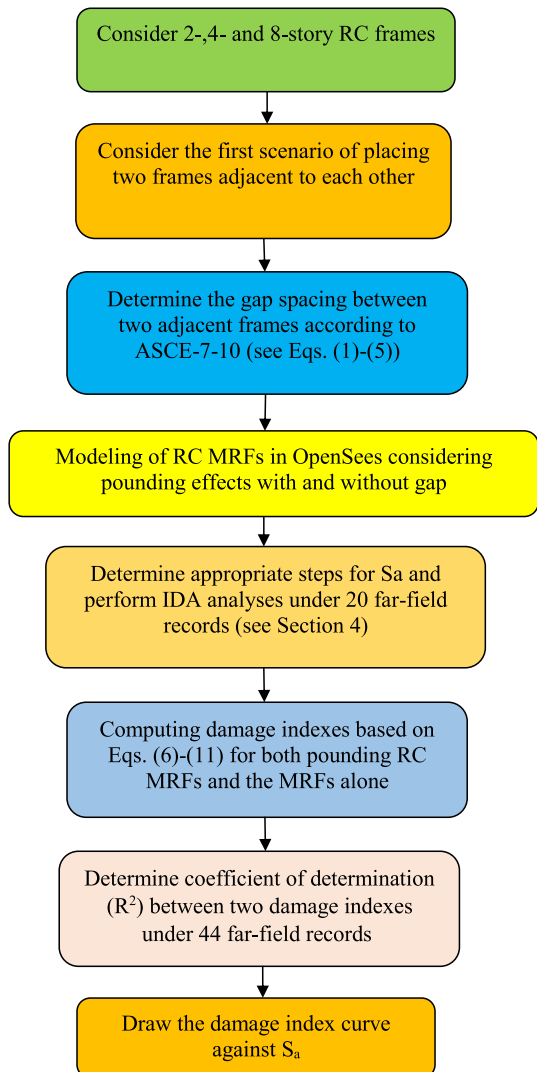
$$DI = \frac{\theta_m - \theta_y}{\theta_u - \theta_y} + \beta \frac{E_h}{M_y \theta_u} \tag{11}$$

where  $\theta_m$  is the maximum experienced rotation of an element in a system subjected to an earthquake,  $\theta_y$  is the yield rotation under monotonic loading,  $\theta_u$  is the ultimate rotation under monotonic loading,  $E_h$  is the hysteretic energy dissipated by the element,  $M_y$  is the

yield moment and  $\beta$  is a parameter calibrated in accordance with experiments to reflect the effect of repeated loading. In this paper,  $\beta$  was assumed to be 0.15 for LS (Kunnath et al. 1992; Reinhorn et al. 2009).

The flowchart of the analysis is shown in Fig. 4.

Fig. 4 Analysis flowchart



## 6 Verification

### 6.1 Estimating the fundamental period of the MRFs

In order to verify the fundamental period of the simulated models, the Numerical algorithms for Subspace State Space System Identification (N4SID) method, as candidate of system identification methods, along with stabilization diagram and Power Spectral Density (PSD), was employed to determine the modal parameters (i.e., natural frequency, damping ratio, and mode shapes). It is worth mentioning that in this method, acceleration responses recorded at the roof of the MRFs under specific ground motion records are selected as output signals, and also the ground motions can be used as input signals. More explanations about the stabilization diagram were presented by Yazdanpanah et al. (2020a, b). In addition, the mathematical relationship of the N4SID method can be found in the literature (Overschee and Moor 1994; Kim and Lynch 2012). As it can be observed in Fig. 5, the fundamental period of the 4-story RC MRF could be estimated as  $T_1 = 1/f_1 = 1/0.895 = 1.1173$  (sec), which accurately matches with the fundamental period obtained by OpenSees, i.e.  $T_1 = 1.1002489$  (sec). Also, Fig. 6 indicates that the first identified period of the 8-story RC MRF is  $T_1 = 1/f_1 = 1/0.620 = 1.6129$  (sec) slightly less than the fundamental period obtained by OpenSees, i.e.  $T_1 = 1.681477$  (sec).

### 6.2 Linear viscoelastic contact element

To justify the impact force between two adjacent frames using the linear viscoelastic contact element, a numerical model was simulated in OpenSees. All the frame models (with and without considering the pounding phenomenon) were studied under the El Centro earthquake using the shaking table (see Fig. 7). Comparison between numerical and experimental results (Khatiwada et al. 2013) indicated that the maximum

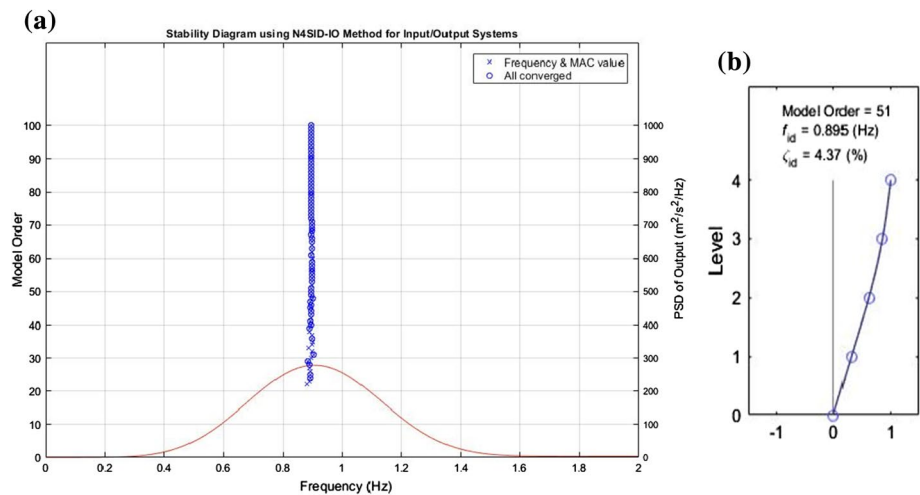


**Fig. 5** Stabilization diagram of the 4-story RC MRF using the N4SID method. **a** stabilization diagram, **b** identified modal parameters

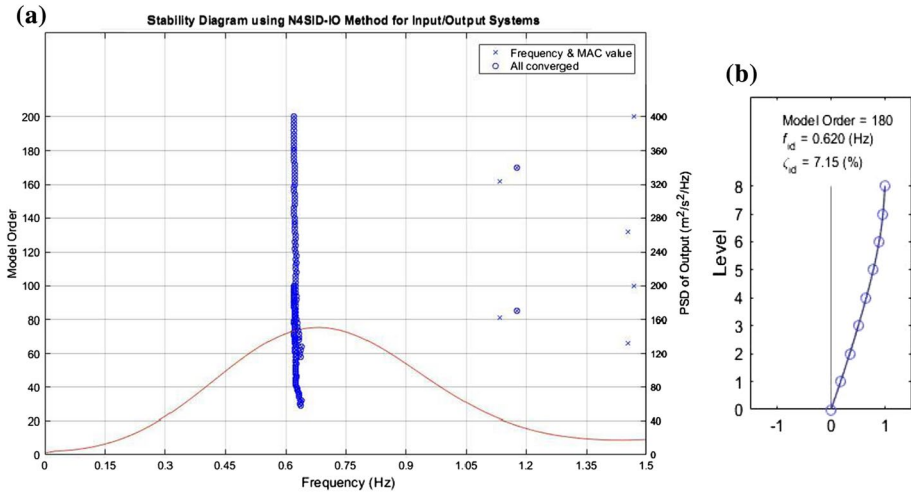


**Fig. 6** The stabilization diagram of the 8-story RC MRF using the N4SID method. **a** stabilization diagram, **b** identified modal parameters

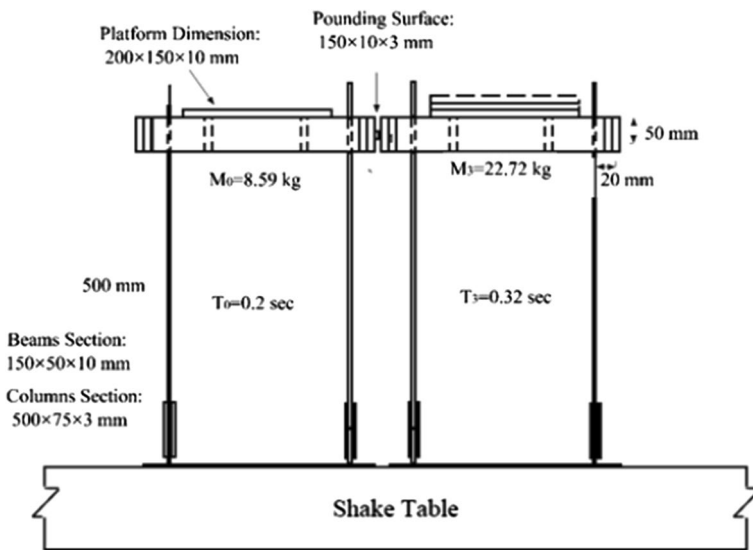


**Fig. 7** Schematic view of the experimental setup (Khawidawa et al. 2013) (CC-BY license, New Zealand Society for Earthquake Engineering)

amplification factor ( $\mu_{max}/u_{max}$ ) for the numerical model was + 1.23 and -1.35 for positive and negative directions, respectively; while these values in the experimental model (Khawidawa et al. 2013) were +1.26 and -1.3 for positive and negative directions, respectively. It is worth mentioning that  $\mu_{max}$  and  $u_{max}$  are the maximum deformations of the reference frame with and without pounding effects, respectively. Therefore, the linear viscoelastic contact element leads to good agreement between numerical and



experimental results and it can be successfully used to study pounding between two adjacent frames.

## 7 Results

### 7.1 Damage Indexes in 2- and 4-story RC MRFs considering pounding effects

Figure 8a, b show the three damage indexes (Park and Ang, modified Park and Ang proposed by Kunnath et al. 1992 and Cosenza et al.) for 2-story RC MRFs considering pounding effects with a minimum separation distance,  $\delta_{MT}$ , as a function of the spectrum acceleration ( $S_a$ ), subjected to ground motions no. 13 and 17 of Table 1, respectively. It should be noted that these *DI*s denote the global damage of the frames. As it can be observed from the figures, all three damage indexes approximately lead to the same results. Based on these results, it can be concluded that the 2-story RC MRF is damaged under ground motions no. 13 and 17 within the range of  $S_a$ :1.1 (g) to  $S_a$ :1.6 (g) and  $S_a$ :1.6 (g) to  $S_a$ :2.1 (g) for the first time. On the other hand, the damage indexes have high values in these steps. It is worth mentioning that the differences between these ranges for the modified Park and Ang damage index under records no. 13 and 17 are larger by about 0.032 and 0.018, respectively, than for the Cosenza et al. damage index. Moreover, the MRF is collapsed under ground motions no. 13 and 17 when  $S_a$ :2.05 (g) to  $S_a$ :2.1 (g) and  $S_a$ :3.2 (g) to  $S_a$ :3.25 (g) (see big changes for these steps).

Figure 9a, b show correlations between the Kunnath et al. damage index and that of Cosenza et al. with minimum separation distance subjected to 44 far-field ground motions that correspond to all beams and columns of the 2-story RC MRF and 4-story RC MRF, respectively. As can be observed from the figures, the coefficients of determination ( $R^2$ ) are very strong and the damage indexes are well correlated.

Based on Fig. 10, it can be concluded that the 4-story RC pounding MRF with minimum separation distance is damaged under ground motions no. 13 and 17 within the range of  $S_a$ :0.6 (g) to  $S_a$ :1.1 (g) for the first time. On the other hand, the damage indexes have high values in this step. Also, the coefficient of determination for the aforementioned damage indexes (presented in Fig. 9b) indicates the high correlation between them. It is worth

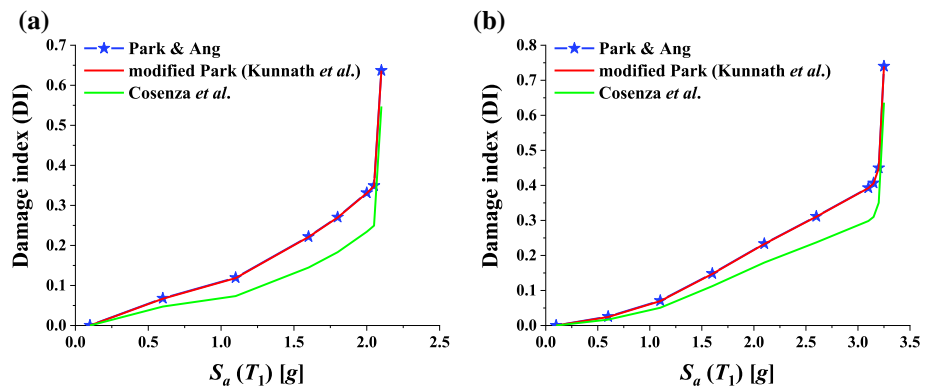
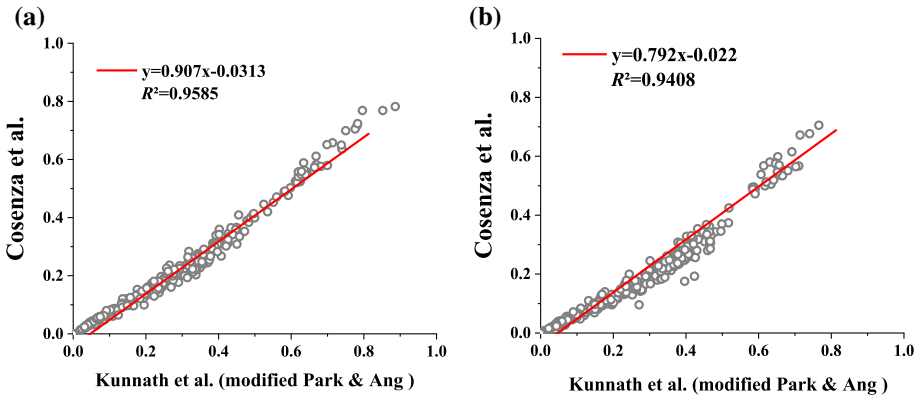
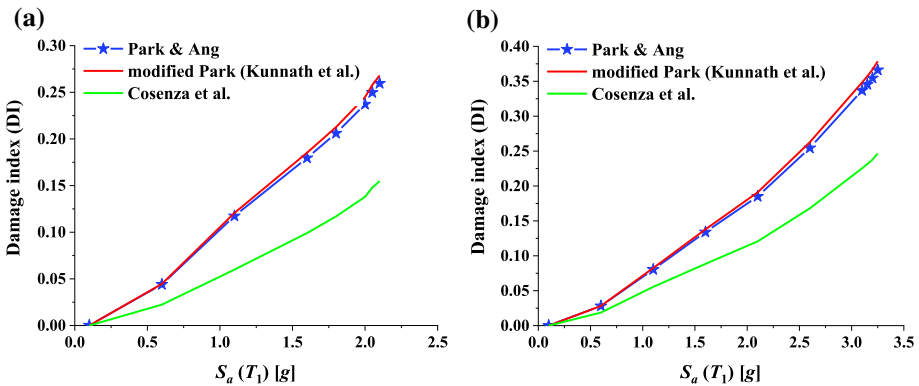


Fig. 8 Comparison of various damage indexes for the 2-story RC MRF considering pounding effect with minimum separation distance subjected to, **a** ground motion no. 13, **b** ground motion no. 17



**Fig. 9** Correlation between the Kunnath et al. damage index and that of Cosenza et al. with minimum separation distance subjected to 44 far-field ground motions that correspond to all beams and columns of the: **a** 2-story RC MRF, **b** 4-story RC MRF



**Fig. 10** Comparison of various damage indexes for the 4-story RC MRF considering pounding effect with minimum separation distance subjected to, **a** ground motion no. 13, **b** ground motion no. 17

mentioning that, the differences between this range for modified Park and Ang damage index under records no. 13 and 17 are larger by about 0.038 and 0.017, respectively than for the Cosenza et al. damage index.

Figure 11a, b present a comparison of various damage indexes for the 2-story RC MRF considering pounding effect without minimum separation distance subjected to ground motion no. 13 and 17, respectively. The results show that the 2-story RC MRF is damaged under ground motions no. 13 and 17 within the range of  $S_a:0.6$  (g) to  $S_a:1.1$  (g) and  $S_a:1.1$  (g) to  $S_a:1.6$  (g) for the first time. On the other hand, the damage indexes have high values in these steps. The differences between these ranges for the modified Park & Ang damage index under records no. 13 and 17 are larger by about 0.029 and 0.014, respectively, than for the Cosenza et al. damage index. Moreover, the MRF is collapsed under ground motions no. 13 and 17 when  $S_a:2.1$  (g) to  $S_a:2.15$  (g) and  $S_a:3.05$  (g) to  $S_a:3.1$  (g) (see the big changes in these steps).

Figure 12a, b show correlations between the Kunnath et al. damage index and that of Cosenza et al. without minimum separation distance subjected to 44 far-field ground



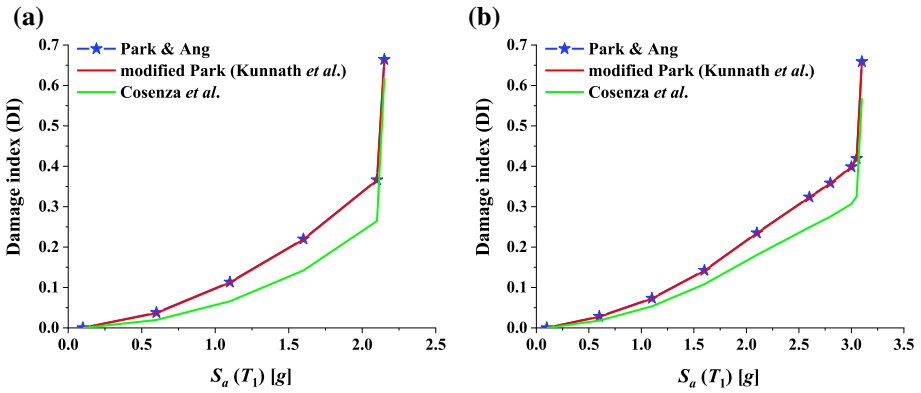


Fig. 11 Comparison of various damage indexes for the 2-story RC MRF considering pounding effect without minimum separation distance subjected to, **a** ground motion no. 13, **b** ground motion no. 17

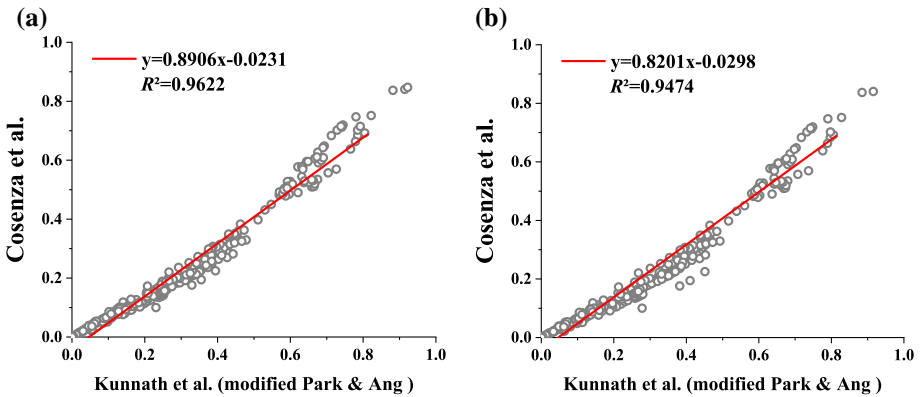


Fig. 12 Correlation between the Kunnath et al. damage index and that of Cosenza et al. without minimum separation distance subjected to 44 far-field ground motions that correspond to all beams and columns of the: **a** 2-story RC MRF, **b** 4-story RC MRF

motions that correspond to all beams and columns of the 2-story RC MRF and 4-story RC MRF, respectively. As it can be observed, the coefficients of determination are very strong and the damage indexes are well correlated.

Based on Fig. 13, it can be concluded that the 4-story RC pounding MRF without minimum separation distance is damaged under ground motions no. 13 and 17 within the range of  $S_a$ : 0.1 (g) to  $S_a$ :0.6 (g) and  $S_a$ :0.6 (g) to  $S_a$ :1.1 (g) for the first time. On the other hand, the damage indexes have high values in this step. Consequently, the differences between these ranges for the modified Park & Ang damage index under records no. 13 and 17 are larger by about 0.031 and 0.015, respectively, than for the Cosenza et al. damage index.

According to the aforementioned results, the modified Park & Ang damage index, due to larger differences for different damage states ( $S_a(T_1)$ ), is more sensitive to seismic damages. Also, the coefficient of determination for the aforementioned damage index is presented in Fig. 12b, which indicates on high correlation. It is worth mentioning that, during pounding between 2- and 4-story RC MRFs, the 4-story has lower values of damage indexes. It means that the 4-story is damaged at lower seismic intensities. In addition, as it



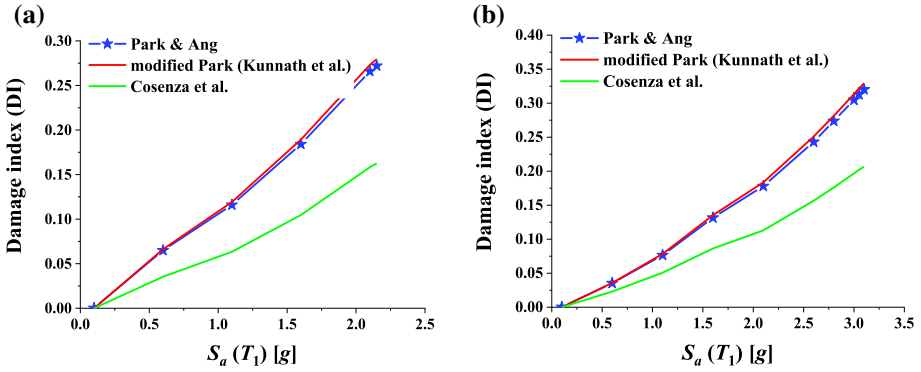


**Fig. 13** Comparison of various damage indexes for the 4-story RC MRF considering pounding effect without minimum separation distance subjected to: **a** ground motion no. 13, **b** ground motion no. 17

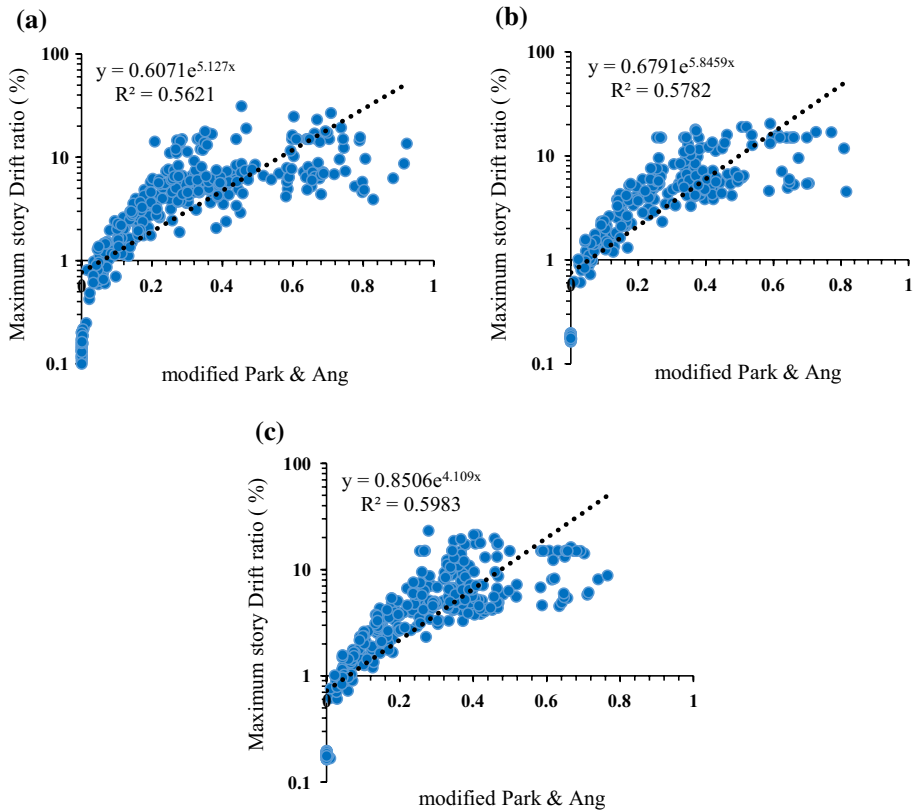


**Fig. 14** Comparison of the coefficient of determination for the 4-story RC MRF subjected to 44 far-field ground motions considering pounding effects: **a** without minimum separation distance **b** with 75% of minimum separation distance, **c** with 100% of minimum separation distance





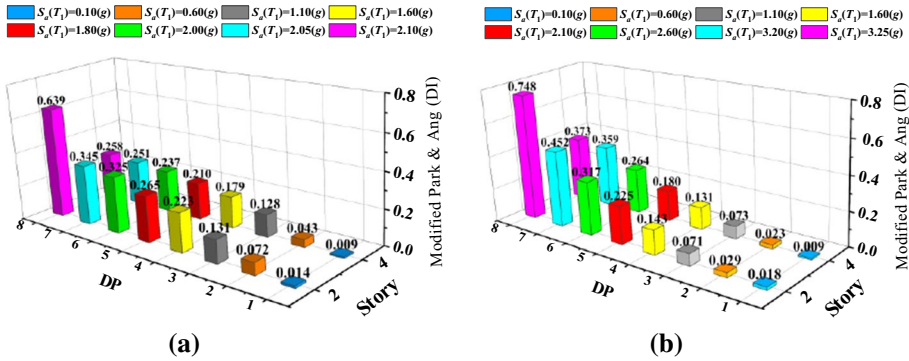


Fig. 15 Comparison of modified Park & Ang damage index for pounding between 2- and 4-story RC MRFs with minimum separation distance subjected to: **a** ground motion no. 13, **b** ground motion no. 17

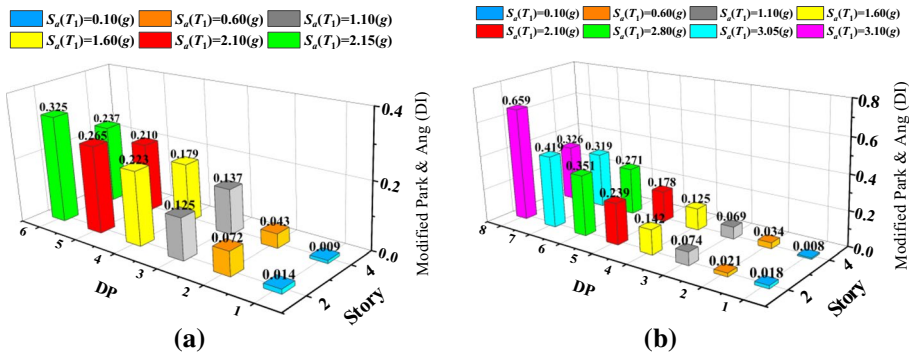
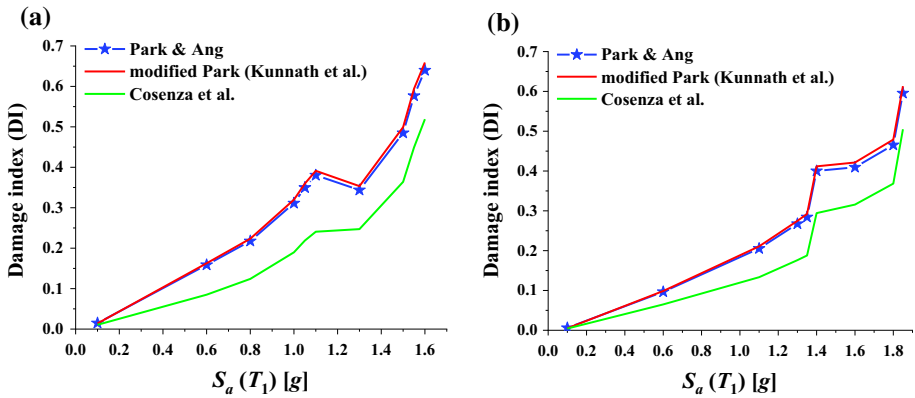


Fig. 16 Comparison of modified Park & Ang damage index for pounding between 2- and 4-story RC MRFs without minimum separation distance subjected to: **a** ground motion no. 13, **b** ground motion no. 17

can be observed from Fig. 14a, b, and c, considering a minimum separation distance,  $\delta_{MT}$ , between two adjacent MRFs (2- and 4-story) leads to an increase in  $R^2$  value for the maximum story drift ratio versus the modified Park & Ang damage index. On the other hand, considering 75% and 100% of  $\delta_{MT}$  improves the  $R^2$  value up to 2.86% and 6.44%, respectively and correlation between these two parameters increases.

Furthermore, comparing the damage indexes for 2- and 4-story RC MRFs considering pounding effect with minimum separation distance (Figs. 8a vs. 10a, 8b vs. 10b) and without minimum separation distance (Figs. 11a vs. 13a, 11b vs. 13b) under the same earthquakes and the same value of  $S_a$ , it can be seen that the damage indexes of the shorter structure are larger than values for the taller structure. In addition, Fig. 15 shows a comparison of modified Park & Ang damage index for pounding between 2- and 4-story RC MRFs with minimum separation distance subjected to ground motion no. 13 and 17 with the same value of  $S_a$ . Moreover, a comparison of modified Park & Ang damage index for pounding between 2- and 4-story RC MRFs without minimum separation distance subjected to ground motion no. 13 and 17 with the same value of  $S_a$ , is presented in Fig. 17. The results shown in both figures (Figs. 16 and 17) confirm that the shorter structure with smaller value of natural period will suffer more extensive damages due to structural pounding.



**Fig. 17** Comparison of various damage indexes for the 4-story RC MRF considering pounding effect with minimum separation distance subjected to **a** ground motion no. 13, **b** ground motion no. 17

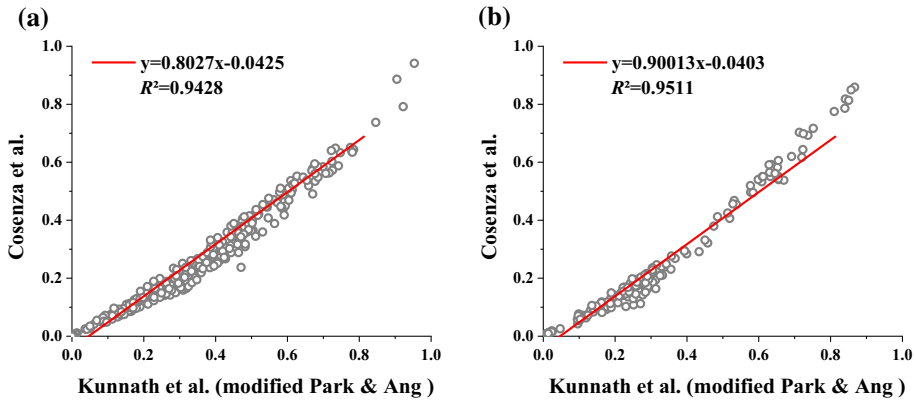
## 7.2 Damage indexes in 4- and 8-story RC MRFs considering pounding effects

Figure 17a and b show the three damage indexes (Park & Ang, modified Park & Ang proposed by Kunnath et al. (1992) and Cosenza et al.) for 4-story RC MRFs considering pounding effects with a minimum separation distance as a function of the spectrum acceleration ( $S_a$ ), subjected to ground motions no. 13 and 17 of Table 1, respectively. It should be noted that these *DI*s denote global damage of the frames. As it can be observed from the figures, all three damage indexes lead approximately to the same results. Based on these results, it can be concluded that the 4-story RC MRF is damaged under ground motions no. 13 and 17 within the range of  $S_a$ :0.1 (g) to  $S_a$ :0.6 (g) and  $S_a$ :0.1 (g) to  $S_a$ :0.6 (g) for the first time. On the other hand, the damage indexes have high values in these steps. It is worth mentioning that, the differences between this range for the modified Park & Ang damage index under records no. 13 and 17 are larger by about 0.074 and 0.033, respectively, than for the Cosenza et al. damage index. Moreover, the MRF is collapsed under ground motions no. 13 and 17 when  $S_a$ :1.3 (g) to  $S_a$ :1.5 (g) and  $S_a$ :1.35 (g) to  $S_a$ :1.40 (g) (see the big changes in these steps).

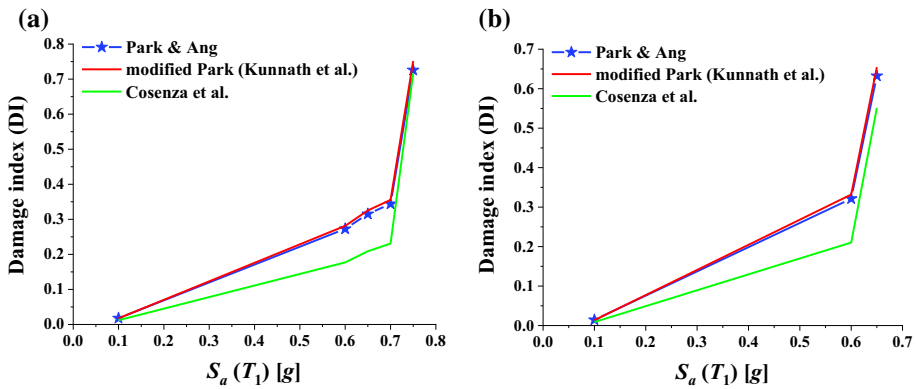
Figure 18a and b show correlations between the Kunnath et al. damage index and that of Cosenza et al. with minimum separation distance subjected to 44 far-field ground motions that correspond to all beams and columns of the 4-story RC MRF and 8-story RC MRF, respectively. As it can be observed, the coefficients of determination are very strong and the damage indexes are well correlated.

Based on Fig. 19, it can be concluded that the 8-story RC pounding MRF with a minimum separation distance is damaged under ground motions no. 13 and 17 within the range of  $S_a$ :0.1 (g) to  $S_a$ :0.6 (g) for the first time. On the other hand, the damage indexes have high values in this step. The differences between this range for the modified Park & Ang damage index under records no. 13 and 17 are larger by about 0.099 and 0.117, respectively, than for the Cosenza et al. damage index. Moreover, the MRF is collapsed under ground motions no. 13 and 17 when  $S_a$ :0.7 (g) to  $S_a$ :0.75 (g) and  $S_a$ :0.6 (g) to  $S_a$ :0.65 (g) (see the big changes in these steps). Also, the coefficients of determination for the aforementioned damage index are presented in Fig. 23c, which indicates on high correlation.





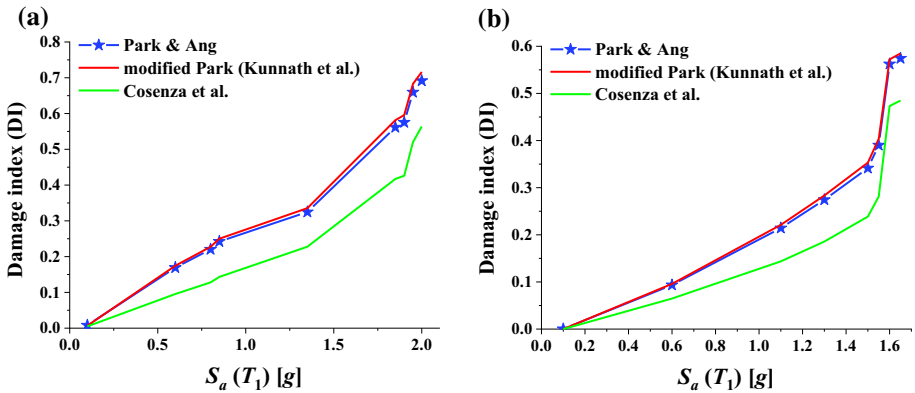
**Fig. 18** Correlation between the Kunnath et al. damage index and that of Cosenza et al. with minimum separation distance subjected to 44 far-field ground motions that correspond to all beams and columns of the: **a** 4-story RC MRF, **b** 8-story RC MRF



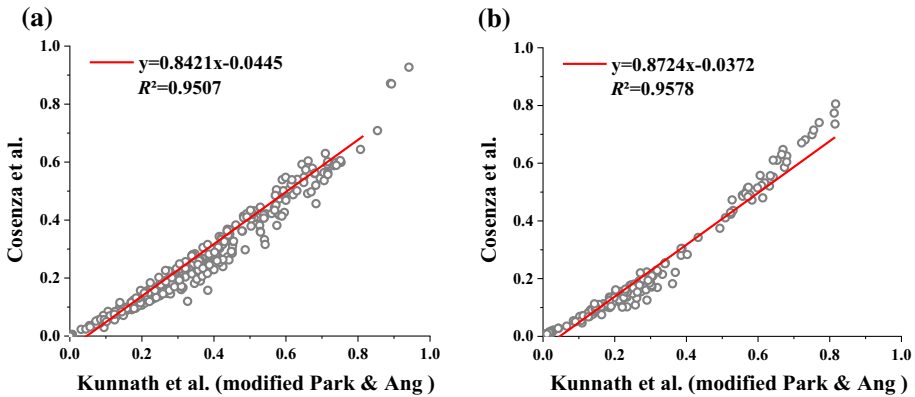
**Fig. 19** Comparison of various damage indexes for the 8-story RC MRF considering pounding effect with minimum separation distance subjected to, **a** ground motion no. 13, **b** ground motion no. 17

Figure 20a and b present a comparison of various damage indexes for the 4-story RC MRF considering pounding effect without a minimum separation distance subjected to ground motion no. 13 and 17, respectively. The results show that the 4-story RC MRF is damaged under ground motions no. 13 and 17 within the range of  $S_a:0.1$  (g) to  $S_a:0.6$  (g) and  $S_a:0.1$  (g) to  $S_a:0.6$  (g) for the first time. On the other hand, the damage indexes have high values in these steps. It is worth mentioning that, the differences between this range for the modified Park & Ang damage index under records no. 13 and 17 are larger by about 0.077 and 0.031, respectively, than for the Cosenza et al. damage index. It is worth noting that pounding between two adjacent MRFs leads to a decrease in the intensity of an earthquake. On the other hand, the MRF is damaged under lower seismic intensities than the state of pounding with minimum separation distance. Therefore, considering a minimum separation distance based on ASCE seismic criteria is necessary.

Figure 21a and b show correlations between the Kunnath et al. damage index and that of Cosenza et al. without a minimum separation distance subjected to 44 far-field ground



**Fig. 20** Comparison of various damage indexes for the 4-story RC MRF considering pounding effect without minimum separation distance subjected to: **a** ground motion no. 13, **b** ground motion no. 17



**Fig. 21** Correlation between the Kunnath et al. damage index and that of Cosenza et al. without minimum separation distance subjected to 44 far-field ground motions that correspond to all beams and columns of the: **a** 4-story RC MRF, **b** 8-story RC MRF

motions that correspond to all beams and columns of the 8-story RC MRF and 4-story RC MRF, respectively. As it can be observed, the coefficients of determination are very strong and the damage indexes are well correlated.

Based on Fig. 22, it can be concluded that the 8-story RC pounding MRF without a minimum separation distance is damaged under ground motions no. 13 and 17 within the range of  $S_a:0.1$  (g) to  $S_a:0.6$  (g) for the first time. On the other hand, the damage indexes have high values in this step. It is worth mentioning that, the differences between this range for the modified Park & Ang damage index under records no. 13 and 17 are larger by about 0.026 and 0.028, respectively, than for the Cosenza et al. damage index Fig. 23. Also, the coefficients of determination for the aforementioned damage index are presented in Fig. 24d, which indicates on high correlation. Like 4-story MRF considering pounding effect without a minimum separation distance, pounding between two adjacent MRFs leads to the decrease in the intensity of an earthquake. On the other



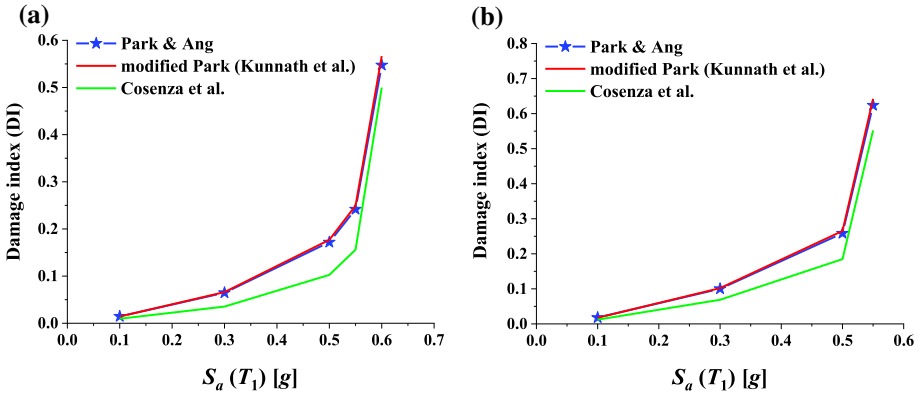


Fig. 22 Comparison of various damage indexes for the 8-story RC MRF considering pounding effect without minimum separation distance subjected to, **a** ground motion no. 13, **b** ground motion no. 17

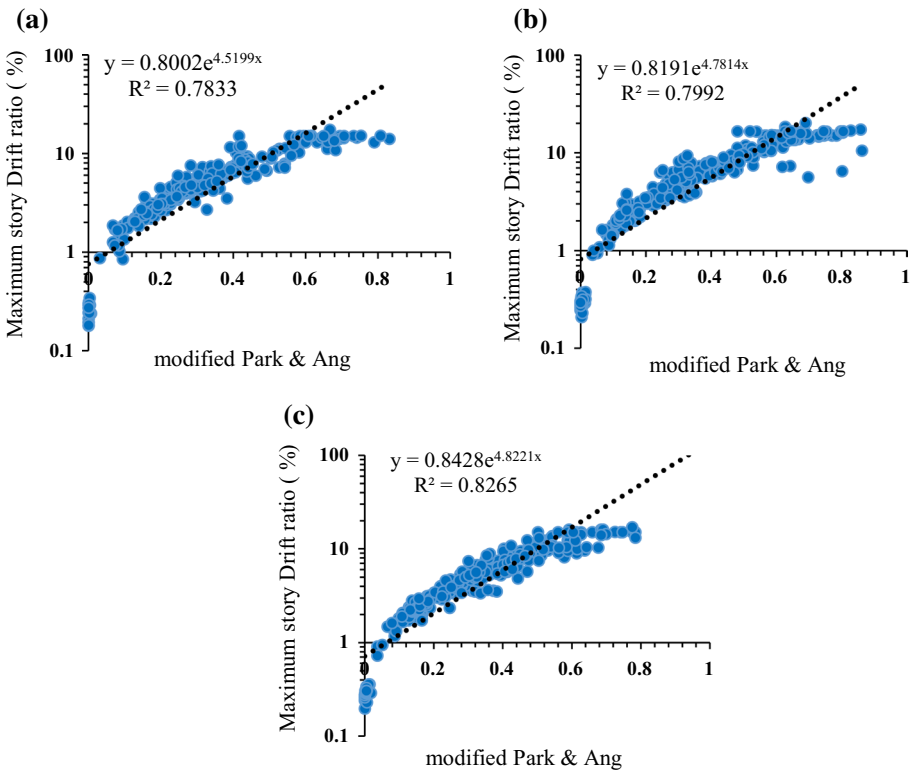
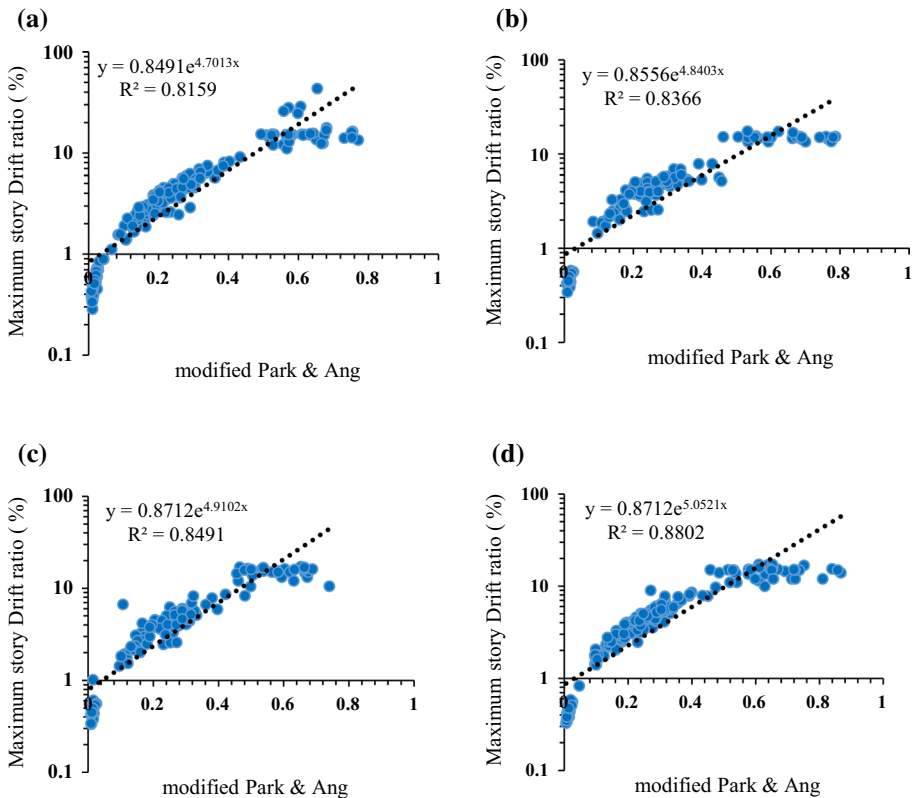


Fig. 23 Comparison of the coefficient of determination for the 4-story RC MRF subjected to 44 far-field ground motions considering pounding effects: **a** without minimum separation distance **b** with 60% of minimum separation distance, **c** with 100% of minimum separation distance



**Fig. 24** Comparison of the coefficient of determination for the 8-story RC MRF subjected to 44 far-field ground motions considering pounding effects: **a** without minimum separation distance **b** with 60% of minimum separation distance **c** with 75% of minimum separation distance, **d** with 100% of minimum separation distance

hand, the MRF is damaged under lower seismic intensities than the state of pounding with a minimum separation distance. Therefore, considering a minimum separation distance leads to the improvement of the situation. Furthermore, comparing the damage indexes for 4- and 8-story RC MRFs considering pounding effect with minimum separation distance (Figs. 17a vs. 19a, 17b vs. 19b) and without minimum separation distance (Figs. 20a vs. 22a, 20b vs. 22b) under the same earthquakes and the same value of  $S_a$ , it can be seen that the damage indexes of the shorter structure are larger than values for the taller structure.

According to the aforementioned results, the modified Park & Ang damage index, due to larger differences for different damage states ( $S_a(T_1)$ ), is more sensitive to seismic damages. In addition, as it can be observed from Figs. 23 and 24 considering a minimum separation distance between two adjacent MRFs (4- and 8-story) leads to the increase in the  $R^2$  value of maximum story drift ratio versus the modified Park & Ang damage index. On the other hand, considering 60% and 100% of  $\delta_{MT}$  for the 4-story RC MRF improves the  $R^2$  value up to 2.03% and 5.51%, respectively. In addition, considering 60%, 75% and 100% of  $\delta_{MT}$  for the 8-story RC MRF improves the  $R^2$  value up to 2.54%, 4.06% and 7.88%, respectively, and the correlation between these two parameters increases.

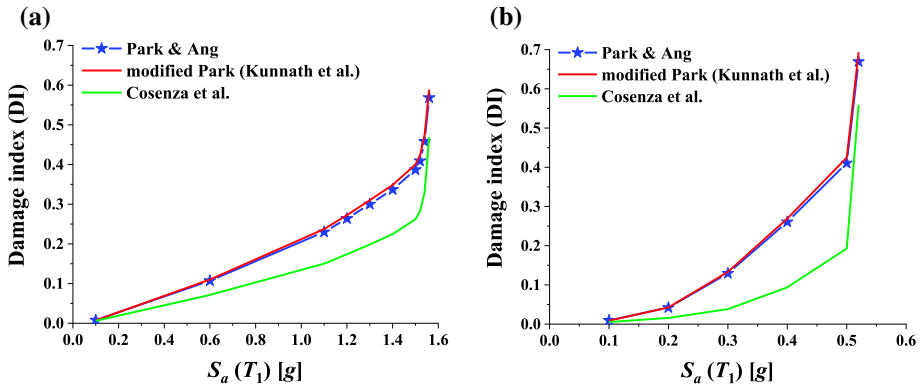


Fig. 25 Comparison of various damage indexes for the 4-story RC MRF (alone) subjected to, **a** ground motion no. 13, **b** ground motion no. 17

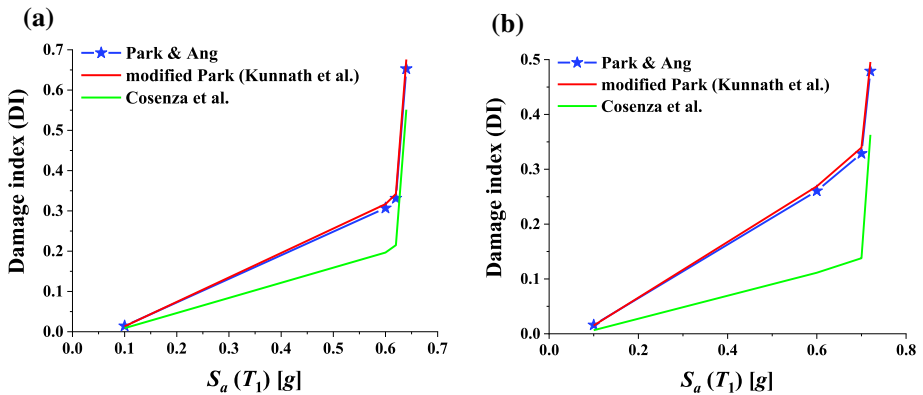


Fig. 26 Comparison of various damage indexes for the 8-story RC MRF (alone) subjected to, **a** ground motion no. 13, **b** ground motion no. 17

Comparison of the results for 4- and 8-story MRFs without pounding effects (independent vibrations) with those considering pounding show that the behavior of the MRFs considering pounding effects with a minimum separation distance are near to those of MRFs without pounding effects. This issue leads to a more accurate prediction of the behavior of MRFs (see Fig. 25 and 26 and compare with those of pounding effects in the previous sections).

### 8 Conclusions

In this article, three damage indexes have been considered for nonlinear damage detection in adjacent RC structures considering pounding effects. Some illustrative benchmark structures including 2- and 4-story as well as 4- and 8-story RC MRFs have been analyzed using IDA analyses under 44 far-field earthquake records. Pounding between RC MRFs has been considered with 60%, 75%, and 100% of the minimum separation distance and compared

to the case when structures vibrate independently. The following conclusions can be drawn from the study:

- Comparison of the results between the MRFs with and without considering pounding effects show that collisions lead to a decrease in the values of coefficient of determination and the nonlinear damage occurs under lower seismic intensity.
- Considering a smaller separation distance leads to an increase in the value of the coefficient of determination.
- The first nonlinear damage, and also the state of collapse, can be detected at the specified seismic intensity.
- Due to larger differences for different damage states, the modified Park & Ang damage index is more sensitive to seismic damages and this damage index also shows larger values, as compared to other damage indicators. On the other hand, it can be concluded that while the trend of changes in all three damage indexes is similar, the modified Park & Ang damage index is on average 28.5% larger than the Cosenza damage index and 3.7% larger than the Park & Ang damage index.
- Considering the minimum separation distance between two adjacent MRFs leads to an increase in the value of the coefficient of determination for the maximum story drift ratio versus modified Park & Ang damage index. Also, by increasing the separation distance between two adjacent structures from 0 to 100% of the minimum separation distance, the damage index is generally decreased.
- By examining and comparing the values of the damage index for different separation distances between two adjacent MRFs, it can be observed that the rate of a variety of the damage index is low and insufficient in the range of 0% to 75% of the minimum separation distance. On the other hand, the maximum reduction in the damage index is in the range of 75% to 100% of the minimum separation distance. These results emphasize the importance and necessity of considering the minimum separation distances between two adjacent MRFs so as to reduce the damages.
- Due to pounding, shorter RC MRFs are damaged more significantly than the taller structures. On the other hand, the shorter RC MRFs (structures with smaller natural period) have high values of damage indexes.

**Funding** No funding was obtained.

**Code availability** Not applicable.

## Declarations

**Conflict of interest** The authors declare no conflict of interest.

**Data availability** Paper contains all data used in the study.

**Open Access** This article is licensed under a Creative Commons Attribution 4.0 International License, which permits use, sharing, adaptation, distribution and reproduction in any medium or format, as long as you give appropriate credit to the original author(s) and the source, provide a link to the Creative Commons licence, and indicate if changes were made. The images or other third party material in this article are included in the article's Creative Commons licence, unless indicated otherwise in a credit line to the material. If material is not included in the article's Creative Commons licence and your intended use is not





permitted by statutory regulation or exceeds the permitted use, you will need to obtain permission directly from the copyright holder. To view a copy of this licence, visit <http://creativecommons.org/licenses/by/4.0/>.

## References

- Al-Amawee AH, Salman MM (2006) The ratio between static and dynamic modulus of elasticity in normal and high strength concrete. *J Eng Sustain Dev* 10(2):163–174
- Alhaddad MS, Wazira KM, Al-Salloum YA, Abbas H (2015) Ductility damage indices based on seismic performance of RC frames. *Soil Dyn Earthq Eng* 77:226–237
- Altoontash A (2004) Simulation and damage models for performance assessment of reinforced concrete beam-column joints. Stanford University, Stanford, California
- Anagnostopoulos S, Karamaneas C (2008) Use of collision shear walls to minimize seismic separation and to protect adjacent buildings from collapse due to earthquake-induced pounding. *Earthquake Eng Struct Dynam* 37(12):1371–1388
- Anagnostopoulos SA (1988) Pounding of buildings in series during earthquakes. *Earthquake Eng Struct Dynam* 16(3):443–456
- ASCE, AS (2002) Minimum design loads for buildings and other structures: 21–80
- Baltzopoulos G, Baraschino R, Iervolino I (2019) On the number of records for structural risk estimation in PBEE. *Earthquake Eng Struct Dynam* 48(5):489–506
- Barros RC, Khatami SM (2013) Damping ratios for pounding of adjacent building and their consequence on the evaluation of impact forces by numerical and experimental models. *Mecanica Exp* 22:119–131
- Barros RC, Naderpour H, Khatami SM, Mortezaei AR (2013) Influence of seismic pounding on RC buildings with and without base isolation system subject to near-fault ground motions. *J Rehabil Civil Eng* 1(1):39–52
- Bracci J, Reinhorn A, Mander J, Kunnath SK (1989) Deterministic model for seismic damage evaluation of reinforced concrete structures. *National Center for Earthquake Engineering Research, Technical Report NCEER-89-0033, State University of New York at Buffalo*
- Cosenza E, Manfredi G, Ramasco R (1993) The use of damage functionals in earthquake engineering: a comparison between different methods. *Earthquake Eng Struct Dynam* 22(10):855–868
- Deierlein G, Haselton C (2005) *Benchmarking the Collapse Safety of Code-Compliant Reinforced Concrete Moment Frame Building Systems*. ATC/JSCA US-Japan Workshop on Improvement of Structural Design and Construction Practices, Proceedings of an International Workshop
- DesRoches R, Muthukumar S (2002) Effect of pounding and restrainers on seismic response of multiple-frame bridges. *J Struct Eng* 128:860–869
- Efraimiadou S, Hatziogeorgiou GD, Beskos DE (2013a) Structural pounding between adjacent buildings subjected to strong ground motions. Part I: the effect of different structures arrangement. *Earthquake Eng Struct Dyn* 42(10):1509–1528
- Efraimiadou S, Hatziogeorgiou GD, Beskos DE (2013b) Structural pounding between adjacent buildings subjected to strong ground motions. Part II: the effect of multiple earthquakes. *Earthquake Eng Struct Dyn* 42(10):1529–1545
- Elwardany H, Jankowski R, Seleemah A (2021) Mitigating the seismic pounding of multi-story buildings in series using linear and nonlinear fluid viscous dampers. *Arch Civil Mech Eng* 21(4):137
- Elwardany H, Seleemah A, Jankowski R (2017) Seismic pounding behavior of multi-story buildings in series considering the effect of infill panels. *Eng Struct* 144:139–150
- Elwardany H, Seleemah A, Jankowski R, El-Khoriby S (2019) Influence of soil-structure interaction on seismic pounding between steel frame buildings considering the effect of infill panels. *Bull Earthq Eng* 17(11):6165–6202
- Ghobarah A, Abou-Elfath H, Biddah A (1999) Response-based damage assessment of structures. *Earthquake Eng Struct Dynam* 28(1):79–104
- Goldsmith W (1960) *Impact: The Theory and Physical Behaviour of Colliding Solids*. London, UK: Edward Arnold
- Hanganu AD, Onate E, Barbat AH (2002) A finite element methodology for local/global damage evaluation in civil engineering structures. *Comput Struct* 80(20–21):1667–1687
- Huang W, Zou M, Qian J, Zhou Z (2018) Consistent damage model and performance-based assessment of structural members of different materials. *Soil Dyn Earthq Eng* 109:266–272
- Ibarra LF, Krawinkler H (2005) *Global Collapse of Frame Structures Under Seismic Excitations*: Pacific Earthquake Engineering Research Center Berkeley, CA

- Ibarra LF, Medina RA, Krawinkler H (2005) Hysteretic models that incorporate strength and stiffness deterioration. *Earthquake Eng Struct Dynam* 34(12):1489–1511
- IBC (2003). *International Building Code (IBC)*, International Code Council (ICC). IL, USA
- Jankowski R (2010) Experimental study on earthquake-induced pounding between structural elements made of different building materials. *Earthquake Eng Struct Dynam* 39(3):343–354
- Jankowski R (2012) Non-linear FEM analysis of pounding-involved response of buildings under non-uniform earthquake excitation. *Eng Struct* 37:99–105
- Kamaris GS, Hatzigeorgiou GD, Beskos DE (2013) A new damage index for plane steel frames exhibiting strength and stiffness degradation under seismic motion. *Eng Struct* 46:727–736
- Kandemir-Mazanoglu EC, Mazanoglu K (2017) An optimization study for viscous dampers between adjacent buildings. *Mech Syst Signal Process* 89:88–96
- Kazemi F, Miari M, Jankowski R (2021a) Investigating the effects of structural pounding on the seismic performance of adjacent RC and steel MRFs. *Bull Earthq Eng* 19(1):317–343
- Kazemi F, Mohebi B, Jankowski R (2021b) Predicting the seismic collapse capacity of adjacent SMRFs retrofitted with fluid viscous dampers in pounding condition. *Mech Syst Signal Process* 161:107939
- Khatami SM, Naderpour H, Barros RC, Jankowski R (2019) Verification of formulas for periods of adjacent buildings used to assess minimum separation gap preventing structural pounding during earthquakes. *Adv Civil Eng* 2019:9714939
- Khatiwada S, Chouw N, Butterworth JW (2013) Evaluation of numerical pounding models with experimental validation. *Bull N Z Soc Earthq Eng* 46(3):117–130
- Kim J, Lynch JP (2012) Subspace system identification of support-excited structures—part I: theory and black-box system identification. *Earthquake Eng Struct Dynam* 41(15):2235–2251
- Kunnath SK, Reinhorn AM, Lobo R (1992) IDARC Version 3.0: A program for the inelastic damage analysis of reinforced concrete structures
- Leibovich E, Rutenberg A, Yankelevsky DZ (1996) On eccentric seismic pounding of symmetric buildings. *Earthquake Eng Struct Dynam* 25:219–233
- Lignos DG, Krawinkler H (2010) Deterioration modeling of steel components in support of collapse prediction of steel moment frames under earthquake loading. *J Struct Eng* 137(11):1291–1302
- Lopez-Garcia D, Soong T (2009a) Assessment of the separation necessary to prevent seismic pounding between linear structural systems. *Probab Eng Mech* 24(2):210–223
- Lopez-Garcia D, Soong T (2009b) Evaluation of current criteria in predicting the separation necessary to prevent seismic pounding between nonlinear hysteretic structural systems. *Eng Struct* 31(5):1217–1229
- Mahmoud S, Jankowski R (2009) Elastic and inelastic multi-storey buildings under earthquake excitation with the effect of pounding. *J Appl Sci* 9(18):3250–3262
- Mahmoud S, Chen X, Jankowski R (2008) Structural pounding models with Hertz spring and nonlinear damper. *J Appl Sci* 8(10):1850–1858
- Mahmoud S, Jankowski R (2011) Modified linear viscoelastic model of earthquake-induced structural pounding. *Iran J Sci Technol Trans Civil Eng* 35:51–62
- McKenna F, Fenves G, Filippou F (2010) *OpenSees*. University of California, Berkeley
- Miari M, Choong KK, Jankowski R (2019) Seismic pounding between adjacent buildings: Identification of parameters, soil interaction issues and mitigation measures. *Soil Dyn Earthq Eng* 121:135–150
- Miari M, Choong KK, Jankowski R (2021) Seismic pounding between bridge segments: a state-of-the-art review. *Arch Comput Methods in Eng* 28(2):495–504
- Mohebi B, Chegini AHT, Miri ART (2019) A new damage index for steel MRFs based on incremental dynamic analysis. *J Constr Steel Res* 156:137–154
- Moustafa A, Mahmoud S (2014) Damage assessment of adjacent buildings under earthquake loads. *Eng Struct* 61:153–165
- Muthukumar S, DesRoches R (2006) A Hertz contact model with non-linear damping for pounding simulation. *Earthquake Eng Struct Dynam* 35(7):811–828
- Naderpour H, Barros RC, Khatami SM (2015) A study of pounding to simulate impact and determine the impact damping ratio. In: Paper presented at the proceedings of the fifteenth international conference on civil. Structural and Environmental Engineering Computing, Prague, Czech Republic
- Naderpour H, Barros RC, Khatami SM, Jankowski R (2016) Numerical study on pounding between two adjacent buildings under earthquake excitation. *Shock Vib* 2016:1504783
- Naderpour H, Khatami SM (2015) A new model for calculating the impact force and the energy dissipation based on CR-factor and impact velocity. *Scientia Iranica* 22(1):59–68
- Naderpour H, Khatami SM, Barros RC (2017) Prediction of critical distance between two MDOF systems subjected to seismic excitation in terms of artificial neural networks. *Period Polytech Civil Eng* 61(3):516–529

- Nie GN, Zhang C-X, Zhi X-D, Dai J (2017) Damage quantification, damage limit state criteria and vulnerability analysis for single-layer reticulated shell. *Thin-Walled Struct* 120:378–385
- Overschee PV, Moor BD (1994) N4SID: subspace algorithms for the identification of combined deterministic-stochastic systems. *Automatica* 30(1):75–93
- Pang R, Xu B, Kong X, Zou D (2018) Seismic fragility for high CFRDs based on deformation and damage index through incremental dynamic analysis. *Soil Dyn Earthq Eng* 104:432–436
- Park Y-J, Ang AH-S (1985) Mechanistic seismic damage model for reinforced concrete. *J Struct Eng* 111(4):722–739
- Polycarpou PC, Papaloizou L, Komodromos P (2014) An efficient methodology for simulating earthquake-induced 3D pounding of buildings. *Earthquake Eng Struct Dynam* 43(7):985–1003
- Reinhorn A, Roh H, Sivaselvan M, Kunnath S, Valles R, Madan A, Park Y (2009) IDARC 2D version 7.0: user's guide of a program for the inelastic damage analysis of buildings. *Buffalo, New York*
- Rezaei H, Moayyedi SA, Jankowski R (2020) Probabilistic seismic assessment of RC box-girder highway bridges with unequal-height piers subjected to earthquake-induced pounding. *Bull Earthq Eng* 18(4):1547–1578
- Rosenblueth E, Meli R (1986) The 1985 Mexico earthquake. *Concr Int* 8(5):23–34
- Ruangrassamee A, Kawashima K (2001) Relative displacement response spectra with pounding effect. *Earthquake Eng Struct Dynam* 30:1511–1538
- Sharifi A, Banan M-R, Banan M-R (2012) A strain-consistent approach for determination of bounds of ductility damage index for different performance levels for seismic design of RC frame members. *Eng Struct* 37:143–151
- Sohtysik B, Jankowski R (2013) Non-linear strain rate analysis of earthquake-induced pounding between steel buildings. *Int J Earth Sci Eng* 6(3):429–433
- Sohtysik B, Jankowski R (2015) Building damage due to structural pounding during earthquakes. *J Phys: Conf Ser* 628:012040
- Sohtysik B, Jankowski R (2016) Earthquake-induced pounding between asymmetric steel buildings. *Seismic Behaviour and Design of Irregular and Complex Civil Structures II, Geotechnical, Geological and Earthquake Engineering* 40 255–261
- Tubaldi E, Barbato M, Ghazizadeh S (2012) A probabilistic performance-based risk assessment approach for seismic pounding with efficient application to linear systems. *Struct Saf* 36–37:14–22
- Yaghmaei-Sabegh S, Jalali-Milani N (2012) Pounding force response spectrum for near-field and far-field earthquakes. *Scientia Iranica* 19(5):1236–1250
- Yazdanpanah O, Mohebi B, Yakhchalian M (2020a) Selection of optimal wavelet-based damage-sensitive feature for seismic damage diagnosis. *Measurement* 154:107447
- Yazdanpanah O, Mohebi B, Yakhchalian M (2020b) Seismic damage assessment using improved wavelet-based damage-sensitive features. *J Build Eng* 31:101311

**Publisher's Note** Springer Nature remains neutral with regard to jurisdictional claims in published maps and institutional affiliations.

